Non-Mechanically Scanned DFTS

D.F. Murphy and D.A. Flavin

Optics Research Group, Department of Computing, Maths & Physics, Waterford Institute of Technology, Cork Rd., Waterford, Ireland

author email: dominicfmurphy@physics.org

Abstract: Non-mechanically scanned dispersive Fourier transform spectrometry (DFTS) is reported for dispersion-insensitive measurements of thermally-induced change in dispersive group delay; optical path scan lengths of 260μm yield 0.5fs resolution for a dispersive optical sample.

1. Introduction

Fast, accurate and high-resolution measurements of changes in group delay and its dispersion in optically dispersive materials including passive and active optical fiber components are of significant importance for both linear and nonlinear processes in telecommunications network devices.

Dispersive Fourier transform spectrometry (DFTS) has been reported for high-accuracy, high-resolution measurements of group delay, thickness, index and dispersion of thick and dispersive samples in mechanically scanned low-coherence interferometer configurations [1-3], overcoming dispersion-induced limitations of centroid based approaches. In the work reported here, DFTS is applied to the high-resolution measurement of small changes in dispersive group delay using a low-coherence non-mechanically scanned interferometer with the potential for large measurement bandwidth. In demonstration of the technique, thermally-induced delay changes applied to an optically thick and dispersive BK7 glass sample are measured.

2. Interferometer Configuration & Measurements

Referring to Figure 1, light from each of a tungsten filament bulb and HeNe laser are co-launched into a single-mode fiber lead, ensuring good spatial coherence and alignment of both sources in the illumination of the non-mechanically scanned interferometer. The spatially composite beam emergent at angle-cleaved port AC is collimated by lens L and illuminates the interferometer with a ~20mm diameter beam. A broadband cube beamsplitter BS of side 25mm splits the beam 50/50 between arms A1 and A2 of the interferometer.

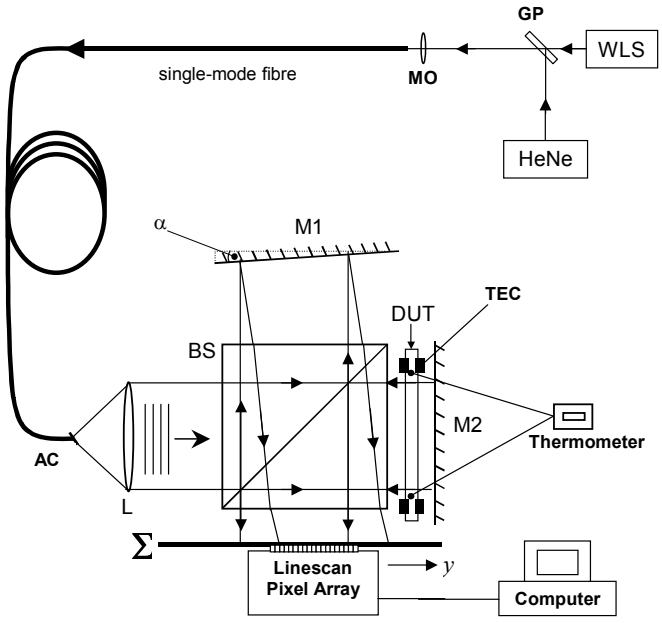

Figure 1: Experimental configuration used for the measurement of thermally-induced dispersive delay change. WLS, white light source; HeNe, Helium-Neon gas laser; GP, glass plate; MO, microscope objective; AC, angled cleave; L, collimating lens; BS, beamsplitter; M1, M2, mirrors; α, mirror tilt angle; DUT, device under test; TEC, thermo-electric cooler; Σ, plane of detection.

Both the device under test DUT (~4mm thick BK7 sample) and mirror M2 are set orthogonal to the incident beam while mirror M1 is tilted about a horizontal angle α. Recombination of the spatially separated beams at BS therefore produces a spatial fringe pattern between the interfering wavefronts, reflected from mirrors M1 and M2, at the output of the interferometer. Provided the optical path delay is within the source coherence length, a straight-line vertical interferogram is formed at the output in the detector plane Σ where it is detected using a 2048 pixel CCD line-scan array, captured and stored on PC for post-processing. Each pixel measures 14μm wide by 200μm long, has a spectral range of 200nm to 1000nm, and a quantum efficiency rating of 50% at 550nm, reducing to only 15% at 850nm.

The optical path scan length may be derived from the wavelength of the illuminating source and the tilt angle applied to the mirror. Further, a relationship between the spatial distribution of the fringes in the direction of the detector array y, and the delay τ between the interfering beams may also be easily determined. For ideal components and in the small angle limit, then $\tau = ky + \tau_c$, where k is a geometric constant and τ_c is the optical delay at the (arbitrary) origin on the detector. In the real case, however, where ideal components and surfaces cannot be assumed, and a non-negligible value of α is required to achieve a scan of the optical path delay, a high-coherence HeNe laser source is used to calibrate τ versus y. Each delay measurement is referenced to the CCD array defined delay origin. Power spectra recovered from HeNe reference interferograms exhibit high spectral quality with narrow FWHM linewidths of ~ 3nm. This degree of spectral quality indicates a high level of periodicity in the interferogram and validates the use of the HeNe interferogram for the linear mapping of delay across the pixel array.

With the interferometer balanced to within the coherence length of the WLS, so that the low-coherence interferogram $I(y)$ is located near the centre of the linescan pixel array, the horizontal tilt angle α applied to mirror M1 was set to achieve a sample density of around 5pixels/HeNe fringe, corresponding to a delay value of about 0.4fs/pixel and a spatial optical path scan length of ~260μm. Reference HeNe laser interferograms were used for delay calibration and optical frequency reference. Respective low-coherence interferograms were captured with 800ms exposure times and 12-bit resolution using a frame grabber card for a set of increasing DUT temperatures from room temperature to ~90°C. Signal-to-noise ratios of the low-coherence tungsten interferograms were as low as ~6.5dB.

3. DFTS Processing & Results

Using the relationship between the complex degree of coherence function $\tilde{\gamma}(\tau)$ of a dispersion distorted interferogram, and the Fourier transform of the normalised complex spectrum $\tilde{G}(\omega)\exp[-i\phi(\omega)]$ [4]:

$$\tilde{\gamma}(\tau) = \int_{-\infty}^{\infty} \left\{\tilde{G}(\omega)\exp[-i\phi(\omega)]\right\}\exp[-i\omega\tau]\,\mathrm{d}\omega \qquad (1)$$

where $\phi(\omega)$ is the frequency dependent phase of the light propagating through the dispersive material, the source spectral phase for each low-coherence interferogram was recovered from the arguments of the interferogram's FFT. Frequency dependent phase evolutions were then respectively derived using a phase unwrapping algorithm; values of spectral phase above the noise floor recovered from the low-coherence interferograms were found to range from ~(1.83 to 2.75)Prad/s. The cumulative dispersive group delay imbalance values $\tau(\omega_0)$ were recovered from a Taylor polynomial expansion about the spectral phase a chosen source spectral frequency ω_0, in this case 2.29Prad/s (~823nm). This derivation of delay is possible due to the relationship between cumulative delay imbalance and phase, i.e., $\tau(\omega_0) = \mathrm{d}\phi(\omega_0) / \mathrm{d}\omega$. The sample's cumulative dispersive group delay is measured over the full temperature range and plotted against temperature T. A first-order least squares fit to the measured data, shown in Figure 2 gives a value of 0.223fs/°C for thermally-induced delay change with a root mean square error of < 0.5fs.

Considering thermal modulation of the DUT, as it heats it expands into the surrounding air gap reducing the gap length with increasing DUT temperature. So, for a double-pass of light through the sample, as applies to this non-mechanically scanned interferometer, the temperature dependent change in the optical path resulting from thermal modulation of the glass sample is

$$\frac{\mathrm{d}\tau_s}{\mathrm{d}T} = \frac{2L}{c}\left\{\psi_g + \beta_g\left[N_g - N_a\right]\right\} \qquad (2)$$

where L is the geometric sample thickness, ψ_g is the thermo-optic coefficient, β_g is the linear thermal expansion coefficient and N_g and N_a are respectively the group refractive indices of the sample and air. Using the literature specified value $\psi_g = 2.6\times10^{-6}$ /°C [9], and the manufacturer specified values of $L = 4.141$mm, $\beta_g = 8.4\times10^{-6}$ /m°C and $N_g = 1.5258$ at the source central frequency of 2.29Prad/s, and a value of 1.000275 for N_a, the expected value of change in dispersive delay for a double-pass through the BK7 sample is 0.194fs for every 1°C increase in temperature, a value that is in good agreement with the experimental result of 0.223fs.

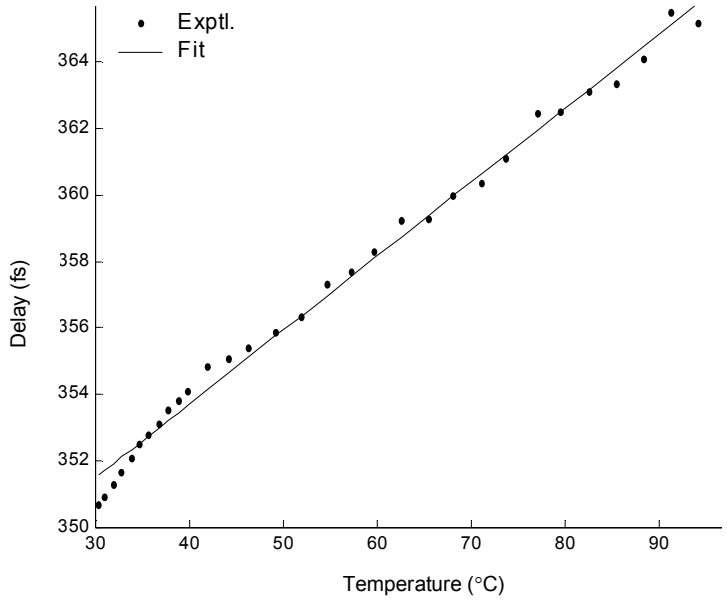

Figure 2: Cumulative group delay values versus temperature for the ~4mm BK7 glass sample placed in the tungsten illuminated interferometer.

4. Discussion

As this work is concerned with measurements of dispersive delay change, not absolute delay, the position of the low-coherence interferogram on the detector array is not critical and the origin of the pixel array may be used as the delay reference point from which measurements of delay change are made. The magnitude of the dispersive imbalance in the interferometer is governed by the degree of tilt applied to the mirror and the physical dimensions and refractive index of the beamsplitter which remain constant during the measurements. Further, as these measurements are of low-level delay modulation (typically < 400 ppm), rather than of absolute cumulative delay, there is a strong common-mode rejection of these dispersive effects.

5. References

[1] P. L. Francois, F. Alard and M. Monerie, "Chromatic Dispersion Measurement from Fourier Transform of White-Light Interference Patterns", Electron. Lett. **23** 357–358 (1987).

[2] B. L. Danielson and C. Y. Boisrobert, "Absolute optical ranging using low coherence interferometry", Appl. Opt. **30** 2975–2979 (1991).

[3] D. F. Murphy and D. A. Flavin, "Dispersion-insensitive measurement of thickness and group refractive index by low-coherence interferometry", Appl. Opt. **39** 4607–4615 (2000).

[4] D.A. Flavin, R. McBride and J.D.C. Jones, "Interferometric fiber-optic sensing based on the modulation of group delay and first order dispersion: application to strain temperature measurand", J. Lightwave Technol. **13** 1314-1323 (1995).